Expression analysis of oncogene transcript in human Aberrant Crypt foci, in comparison to the normal colonic mucosa and colorectal carcinoma from formalin-fixed paraffin-embedded tissue samples: A Pilot Study

Mohamed Sulaiman
All India Institute of Medical Sciences
Jayati Sarangi
All India Institute of Medical Sciences
Aijaz Ahmed
All India Institute of Medical Sciences
Shouriyo Ghosh
All India Institute of Medical Sciences
Lailta Mehra
All India Institute of Medical Sciences
Brijnandan Gupta
All India Institute of Medical Sciences
Ashish Datt Upadhyay
All India Institute of Medical Sciences
Sujoy Pal
All India Institute of Medical Sciences
Nihar R Dash
All India Institute of Medical Sciences
Vineet Ahuja
All India Institute of Medical Sciences
Rajni Yadav
All India Institute of Medical Sciences
Atul Sharma
All India Institute of Medical Sciences
SVS Deo
All India Institute of Medical Sciences
Siddhartha Datta Gupta
All India Institute of Medical Sciences

PRASENJIT DAS (prasenaiims@gmail.com)
All India Institute of Medical Sciences https://orcid.org/0000-0002-2420-8573

Research Article

Keywords: Aberrant crypt foci (ACF), colorectal carcinoma, pathogenesis, tumor biology, gene expression analysis, Immunohistochemistry

Posted Date: March 14th, 2022

DOI: https://doi.org/10.21203/rs.3.rs-1438861/v1

Abstract

Purpose: Aberrant Crypt Foci (ACF) are microscopic preneoplastic lesions in human colon detectable by magnified chromoendoscopy. Our aim was to analyze the expression of a chosen gene transcript in harvested colonic ACF, corresponding colorectal carcinomas (CRC) and normal mucosa.

Methods: A total of 35 cases having ACF >4 in number/ 4 mm^2 colonic mucosa were selected from 302 fresh colectomy samples screened along with the corresponding CRC (35) and normal colonic mucosal shavings (20). Gene expression analysis was performed by reverse transcriptase-polymerase chain reaction in these 3-groups. The gene expression data were correlated with histological and topographical ACF types, lymph node metastasis, site, size, and stage of tumors.

Results: The *KRAS, CDKN1A, CDKN2A, MLH1, VEGFA, and CCL5* gene expressions were significantly altered in ACF compared to controls (p <0.01), while the genes *CDNK2A, PTEN* (p 0.01), and *SMAD4* (p 0.05) were significantly altered in CRC than in controls. The gene expression profile of the mucosal ACF and corresponding CRC foci were similar. No definitive correlation was found between topographic and histological types of ACF and gene expressions. Up-regulation of *IGF1* and *EGFR* genes in ACF were associated with higher lymph node metastases and larger tumor sizes respectively, while down-regulation of *RB1* and *Bcl2* genes were associated with smaller tumor size.

Conclusions The molecular pathogenesis of ACF is as complex as that like advanced CRC foci. Our observation is fascinating as it brings forth the complex pathogenesis of these early mucosa lesions and defies sequential molecular accumulation hypothesis.

Introduction

According to the Globocan project 2020, colorectal carcinoma (CRC) is the third most common cancer in men and second commonest cancer in women, constituting approximately 10% of all cancer cases worldwide and the second most common cause of cancer-related death in the western world [1]. Worldwide including in South-East Asia, CRC prevalence is increasing due to lifestyle transition and eating behaviour, especially in patients aged < 50 years and is a major cause of mortality and morbidity in these regions [2, 3]. Population-based screening programs are lacking in South Asian region and high-risk first-degree relatives of patients are usually screened electively using the conventional endoscopes. Due to the advent of high magnification chromoendoscopy technique it is now possible to identify early preneoplastic mucosal lesions as aberrant crypt foci (ACF) and to take biopsy samples for further analyses [4, 5]. ACF has been established as the earliest identifiable microscopic mucosal preneoplastic lesions in otherwise normal-looking colonic mucosa [6–8]. Compared to the adjacent normal colonic mucosa, ACF is an elevated, deeply stained group of crypts that have luminal dilatation > 3 times the adjacent normal crypt lumen with a diverse crypt pit pattern (rounded, serrated, and elongated). However, at present, our understanding of ACF is limited and needs further analyses.

The pathogenetic theories of CRC is evolving over last few decades and it is now known that the ACF like mucosal lesions can precede a CRC tumor mass in human colon [4, 5]. In our earlier studies, ACF number, location and topographic patterns were correlated with histological dysplastic changes and carcinogenic markers in human colon [9–11]. Molecular alterations in these microscopic ACF-like lesions have been identified in various published studies [12, 13]. It is an important preposition to investigate the molecular changes in ACF-like lesions including the chromosomal instability (CIN), phenotype of the CpG island methylator (CIMP), microsatellite instability (MSI), growth factor alterations, inflammatory pathways, or activation of stem cell pathways as have been established as important molecular alterations in CRC [14–16]. In this study, we harvested human colonic mucosa after applying methylene blue staining under magnification that showed multiple ACF-like lesions and investigated gene expression analysis of selected oncogene transcripts in the harvested ACF, and compared the corresponding CRC, and the normal colonic mucosa, and correlated the same with the topographic and histological characteristics of these patients.

Methods

Tests and controls:

This ambispective study consisted of 302 fresh colectomy specimens from CRC patients. Random mucosal shaves at least 5 centimetres away from the main tumor mass were analyzed for the presence of ACF-like lesions under 40x magnification, and finally, a total of mucosal patches from 35 patients having ≥ 4 ACFs/ 4cm^2 area were included as the target group. In addition, sections from corresponding tumor mass (n 35) (disease control group), and mucosal shaves from another 20 cases (control group) from colectomies with non-malignant indications as like tuberculosis (n 5), perforation peritonitis (n 8), non-specific organizing serositis (n 1), infectious colitis (n 1), Crohn's disease (n 4) and colonic duplication (n 1) were included. Autolyzed specimens, cases where macroscopically normal-appearing mucosa was not available at least 5 centimetres away from the primary tumor mass, and cases with a history of neoadjuvant therapy were excluded. The study protocol was ethically approved by the Institute's Ethics Committee, memorandum no. IECPG – 243/30.03.2016, RT – 7/27.0.4.2016 dated 28th April 2016.

Sample Processing:

In addition to routine grossing as per standard guidelines, macroscopically normal-looking colonic mucosal flaps (2x2cm^2) were shaved out from two different areas, proximal and distal to tumor mass, at least 5 centimetres away from the tumor mass, and fixed overnight in 10% neutral buffered formalin while pinned over a wax-board.

Identification of ACF:

Following fixation, the flaps were stained with 0.5% methylene blue and observed under 40x magnification of a brightfield microscope keeping the stained mucosal flaps directly over a 1mm thick

glass slide to mimic a chromoendoscopy procedure and were photographed. ACFs were defined as groups of elevated and hyper stained dilated mucosal crypts compared to the surrounding area, having luminal dilatation at least three times the diameter of a normal-sized adjacent crypt. The ACFs on the mucosal flaps were marked with water-resistant Davidson ® tissue red paint for future identification. The representative area of the flaps was cut into thin strips, blocks were processed, and sections cut. Hematoxylin and eosin-stained slides were examined under the microscope for confirmation of the ACF and histological analyses were performed to determine the type of epithelium that lines the ACF. As described above, a total of 35 cases were then selected comprising at least > 4 ACF within 4 cm^2 mucosal area to better represent the sampled tissue for further genetic analysis. Being microscopic preneoplastic lesions, laser dissection of the ACF was not done considering that the paucity of RNA could be extracted thereafter.

Extraction and preparation of RNA and cDNA:

Total RNA was extracted from six 10µm thick sections cut from formalin-fixed mucosal strips with ACF, sections were chosen from the corresponding CRC, and formalin-fixed mucosal sections from control samples using the Qiagen RNAeasy FFPE kit (CAPH 13592, USA) according to the manufacturer's protocol. The final elute was obtained using 30µl of RNAase-free water and assessed for RNA quality and quantity by measuring the absorbance in a Nano-Drop Spectrophotometer (Thermo-Scientific, MA, USA). Samples not having an absorbance of 260/230 > 1.7 and 260/280 > 1.8 were reextracted. After the elution, cDNA was prepared immediately using RT2 first strand kit (cat no. 330401, Qiagen), and the final elute of 20 ul was stored at -20 ºC.

Customization of PCR array for mRNA expression in different genes

From a literature search on the gene expression profile of CRC, we selected a total of 20 genes based on their prevalence, representation of different pathways, and a customized RT2 Profiler PCR Array (96 well plate) was made that was outsourced to Qiagen (Cat no. 330171) (Fig. 1). The following groups of genes were included in this study: Tumor suppressor genes: *APC, TP53*; protooncogene: *KRAS*; Cell cycle regulators: *CDKN1A, CDKN2A, PTEN, SMAD4, RB1;* Anti-apoptotic genes: *BRAF, AKT1*; Pro-apoptotic genes: *FADD, Bcl2*; Mismatch repair genes: *MLH1, MSH2, PMS1*; Growth factor-related genes: *EGFR, VEGFA, IGF1*; and Inflammatory marker genes: *CCL5, CXCR4* (Figs. 2 & 3). *GAPDH* was used to normalize the gene expression, reverse transcriptase control and positive PCR controls were included using a pre-dispensed external DNA template of known copies to produce a defined Ct value under proper PCR conditions.

The cycling profile of the reaction was: 95°C for 15 minutes for 1 cycle to kick start the reaction; followed by amplification (94°C for 15 seconds, 55°C for 30 seconds, and 72°C for 1 minute) for 40 cycles. To ensure a single gene-specific product, we have performed melt curve analyses and agarose gel electrophoresis (2% agarose gel run in 0.5 x TBE and stained with ethidium bromide after each reaction to

verify the specificity of the product obtained (Fig. 4). After the completion of the reaction, Ct values were noted for all the genes in respective with the housekeeping genes and the fold change (ΔΔCt) was calculated.

Internal validation:

To assure quality control, we also performed a melt curve analysis after every reaction, to confirm a single gene-specific amplification product. The PCR reaction mixtures were also run on 2% agarose gel electrophoresis to verify a single PCR product (Fig. 4).

Immunohistochemical validation with gene expression data (selected):

To also validate our gene expression data, we had attempted immunohistochemical (IHC) stains on sections cut from residual FFPE blocks, bearing in mind the limited availability of residual tissue post-sectioning for RNA extraction.

Six immunohistochemical (IHC) markers were performed to validate protein expression with gene expression in cases where the results are interpretable.

1. MMR gene-specific markers (indicating microsatellite instability): MLH1, MSH2, PMS1, MSH6
2. Mutation-specific marker: BRAF V600E
3. Marker of the cell cycle regulator: APC (Adenomatous polyposis coli)

Tissue sections (5 µm) cut from paraffin blocks were deparaffinized. Endogenous peroxidase was blocked using 4% hydrogen peroxide followed by antigen retrieval by boiling. Primary monoclonal antibodies for MLH1 (1:200, ph: 9, BioSB, California, USA), MSH2 (1:500, ph: 6, Spring Bioscience, USA), PMS2 (1:200, Spring Bioscience, USA), BRAF V600E (1:200, ph :6, Spring Bioscience, USA) and APC (1:500, ph :9, Santa Cruz, USA) were used to incubate sections at 4 ° C, in a moist chamber overnight. The reaction product was developed with 3,3”- diaminobenzidine and counterstained with Hematoxylin. Appropriate positive and negative controls were used.

The IHC slides were then evaluated by comparing the staining pattern in ACF, tumor focus, and normal mucosal controls separately, and H scores were determined using the intensity and distribution of each stain (H score = I x D). Though conventionally, nuclear positivity for MMR markers is interpreted as MMR-proficient (MMRp) type and complete absence of nuclear positivity is considered as MMR-deficient (MMRd) type, in this study, for the sake of validating the mean fold-change value of mRNAs studied we calculated the H-scores of each of the IHC staining performed.

Statistical analysis:

Data analysis was carried out using Stata 12.0 software (college station, Texas, USA). Data were represented as mean, median (min-max), and percentage of numbers as appropriate. All continuous

variables were normalized using the Shapiro wills test. Continuous variables were compared using the rank-sum test since the data was following a normal distribution. A p-value of < 0.05 is considered statistically significant.

Results

The basic clinical parameters of patients with multiple ACF and their corresponding colonic tumor tissue (disease control) are as follows: 24 were men (age ranging from 22–76 years) and 11 were women (age ranging from 40–69 years). Eight samples were right hemicolectomies, 7 were low anterior resections, 13 were abdominoperineal resections, 5 were subtotal colectomies, and 2 were rectosigmoid resections. Of the 20 cases included as normal controls, 11 were males (age ranging from 3–68 years) and 9 were females (age ranging from 17–65 years). The topographic and histological details of the ACF are described in Table 1 (Fig. 1).

Table 1
Comparing ACF morphological data between right and left side of colon

Parameters	Right colon	Left colon
Mean ACF number	6–10	9–15
Mean ACF area	2.53 cm^2	2.37cm^2
Multiplicity (mean no.)	2–3	4–7
Presence of lymphoid follicles	Less	More
ACF topography		
Round (n = 19)	7	11
Slit (n = 10)	5	6
Serrated / gyriform (n = 6)	2	4
ACF histology		
Normal (n = 19)	7	12
Hyperplastic (n = 10)	4	6
Dysplastic (n = 6)	2	4

Gene Expression Results:

We analyzed differential gene expressions among three groups included in this study: a) ACF in relation to control, b) CRC in relation to control, and c) ACF in relation to CRC. Up-regulation and down-regulation were considered for genes showing a two-fold increase or decrease in mean fold change in relation to

housekeeping gene expression (*GAPDH*). Out of the whole set of genes, the number of samples which showed gene expression/amplification in ACF, CRC, and normal controls have been highlighted in Table 2. Overall, gene expression analyses failed in 10 of the cases due to the low concentration of RNA extracted from FFPE tiny ACF lesions.

Table 2
Summarizing the significant gene expression results both in ACF and CRC in comparison to controls

	Genes	Control (n)	Mean FC +/- SD (controls)	Median (min–max) controls	ACF (n)	Mean FC +/- SD (ACF)	Median (min – max) ACF	P value (median)
Aberrant Crypt Foci	KRAS	20	1 +/- 1.14	0.75 (0.01–4.7)	17	2.04 +/- 3.69	0.68 (0.01–13.42)	**0.05**
	CDKN1A	20	1 +/- 1.63	0.45 (0.03–5.2)	22	1.51 +/- 2.54	0.55 (0.01–13.1)	**0.01**
	CDKN2A	8	1 +/- 1.63	0.31 (0.05–4.7)	6	43.57+/- 86.8	5.57 (1.11–219.8)	**0.05**
	MLH1	16	1 +/- 0.89	0.92 (0.04–2.9)	10	0.24 +/- 4.64	0.71 (0.01–15.2)	**0.01**
	VEGFA	20	1 +/- 1.38	0.48 (0.02–4.7)	25	0.87 +/- 2.02	0.19 (0.01–9.5)	**0.05**
	CCL5	19	1 +/- 1.61	0.51 (0.03–7.2)	16	0.99 +/- 1.55	0.36 (0.01–4.2)	**0.02**
	Genes	**Control (n)**	**Mean FC +/- SD (controls)**	**Median (min–max) controls**	**CRC (n)**	**Mean FC +/- SD (Tumor)**	**Median (min – max) Tumor**	**P value (median)**
Colorectal Carcinoma	CDKN2A	8	1 +/- 1.63	0.31 (0.05–4.7)	10	3.81 +/- 2.56	3.78 (0.04–7.5)	**0.006**
	PTEN	20	1 +/- 4.06	0.06 (0.01–18.2)	21	0.06 +/- 0.13	0.03 (0.01–0.3)	**0.01**

n = number of cases shows gene expression; FC = Fold change; SD = Standard deviation

	Genes	Control (n)	Mean FC +/- SD (controls)	Median (min–max) controls	ACF (n)	Mean FC +/- SD (ACF)	Median (min – max) ACF	P value (median)
	SMAD4	18	1 +/- 1.36	0.54 (0.01–5.8)	21	0.62 +/- 0.93	0.28 (0.01–4.1)	**0.05**

n = number of cases shows gene expression; FC = Fold change; SD = Standard deviation

Comparison of gene expressions in ACF in relation to normal controls:

In the ACFs studied, the expressions of the *APC, KRAS, CDKN2A, RB1, EGFR, MLH1, and IGF1* gene were up-regulated, while the expressions of the *PTEN, BRAF, BCL2* genes were down-regulated compared to controls (Fig. 2). There was no significant difference in the *TP53, CDKN1A, AKT1, SMAD4, FADD, MSH2, PMS1, VEGFA, CCL5, and CXCR4* gene expressions between the ACF and normal mucosal controls. Among the genes that were up-regulated or down-regulated, the gene expressions of the *KRAS gene expressions (p-value – 0.05), CDKN1A (p-value – 0.01), CDKN2A (p-value – 0.05), MLH1 (p-value – 0.01), VEGFA (p-value – 0.05) and CCL5 (p-value – 0.02)* gene expressions were statistically significant between these two groups of samples (Fig. 2).

Comparison of gene expressions in CRC in relation to normal controls:

In the CRC the *APC, CDKN2A, and FADD* genes were upregulated, while the *KRAS, CDKN1A, PTEN, EGFR, BCL2, VEGFA, and CCL5* gene expressions were downregulated as compared to controls (Fig. 3). The *TP53, AKT1, SMAD4, RB1, BRAF, MLH1, MSH2, PMS1, IGF, and CXCR4* genes did not show differential expression between CRC and normal controls. Among the genes that showed differential expressions, fold changes of *CDKN2A (p-value – 0.01), PTEN (p-value – 0.01), and SMAD4 (p-value – 0.05)* were statistically different in CRC than in controls (Fig. 3).

Comparison of gene expression in ACF in relation to CRC:

Expressions of the *KRAS, CDKN1A, CDKN2A, AKT1, RB1, EGFR, BCL2, MLH1, PMS1, VEGFA, IGF1*, and *CCL5* genes were up-regulated in ACF, while the *BRAF* and *FADD* genes were down-regulated in ACF than in CRC. However, none of the genes studied showed a statistically significant difference in expression compared between the ACF and CRC (Table 2).

Correlation of gene expression in ACF with clinical parameters:

The gene expression profile in ACF was correlated with available clinical information as lymph node metastasis, site, and size of the tumor, tumor stage, histological and topographical types of ACF. Upregulation of *the IGF1* gene was associated with more lymph node metastasis (p-value – 0.05) and higher tumor stages (pT3 and pT4) as compared to tumors with early tumor stages (pT1 and pT2) (p-value – 0.05). Furthermore, up-regulation of the *RB1 genes* (p-value – 0.01) and down-regulation of the *Bcl2 genes* (p-value – 0.01) genes were associated with tumor size < 5cm in diameter, while up-regulation of the *EGFR gene (p-value – 0.01)* gene was associated with increased tumor size. The overexpression of the *AKT1* gene was significantly more identified in the left colonic ACF (p-value – 0.01).

The other genes studied did not show a significant correlation with clinical parameters. Also, topographically the ACFs were classified based on the predominant pit patterns as slit, round, and gyriform/serrated types. Histologically, ACFs were also subclassified according to the presence of normal, hyperplastic, or dysplastic epithelium. These topographic or histological ACF subtypes however did not show a statistically significant correlation of gene expression profiles in this study (Table 3).

Table 3
Clinical correlation of lymph node metastasis with gene expressions in ACF

Lymph node metastasis								
Gene	**Mean FC (ACF)**	**LN (-) (n)**	**Mean FC LN (-) +/- S.D**	**Median (min-max) LN (-)**	**LN (+) (n)**	**Mean FC LN (+) +/- S.D**	**Median (min – max) LN (+)**	**P value (median)**
IGF1	**2.44**	5	0.19 +/- 0.18	0.12 (0.07–0.5)	4	5.24 +/- 9.04	0.95 (0.28–18.7)	0.05
Tumor stage								
Gene	**Mean FC (ACF)**	**lower (n)**	**Mean FC lower +/- S.D**	**Median (min-max) Lower**	**Higher (n)**	**Mean FC higher +/- S.D**	**Median (min – max) Higher**	**P value (median)**
SMAD4	1.11	7	1.82 +/- 4.23	0.23 (0.07–11.4)	4	0.11 +/- 0.13	0.07 (0.01–0.3)	0.05
IGF1	**2.44**	5	0.19 +/- 0.18	0.12 (0.07–0.5)	4	5.24 +/- 9.04	0.95 (0.28–18.7)	0.05
Tumor size								
Gene	**Mean FC (ACF)**	**Size < 5 (n)**	**Mean FC Size < 5 +/- S.D**	**Median (min-max) Size < 5**	**Size > 5 (n)**	**Mean FC Size > 5 +/- S.D**	**Median (min – max) Size > 5**	**P value (median)**
AKT1	**1.66**	**12**	2.53 +/- 3.55	0.82 (0.08–9.9)	7	0.17 +/- 0.19	0.1 (0.01–0.5)	0.01
RB1	**2.03**	13	2.81 +/- 3.64	1.43 (0.04–13.9)	6	0.36 +/- 0.24	0.36 (0.19–2.22)	0.01

ACF = aberrant crypt foci; n = number of cases show gene expression; FC = fold change; LN (-) = no metastasis to lymph node; LN (+) = metastasis to lymph node; S.D = standard deviation

Lymph node metastasis								
EGFR	**2.05**	10	3.36 +/- 5.26	0.77 (0.17–13.9)	17	0.18 +/- 0.14	0.12 (0.01–0.47)	0.006
BCL2	0.16	17	0.22 +/- 0.69	0.01 (0.01–2.8)	8	0.01 +/- 0.03	0.01 (0.01–0.09)	0.05
PMS1	1.68	12	2.43 +/- 3.63	0.67 (0.01 11.5)	6	0.19 +/- 0.19	0.14 (0.01–0.5)	0.01

ACF = aberrant crypt foci; n = number of cases show gene expression; FC = fold change; LN (-) = no metastasis to lymph node; LN (+) = metastasis to lymph node; S.D = standard deviation

Immunohistochemical validation of the expression of selected genes:

Gene expression analysis was carried out in all 90 samples, of which 20 were normal controls and 35 were corresponding ACF and CRC tumor samples, respectively. Among these 35 cases, in 10 cases amplification failed due to a low concentration of RNA yield from FFPE samples. Excluding these 10 cases, IHC studies were performed for the following genes in the rest of the cases: *APC, BRAF, MLH1, MSH2, and PMS1* to correlate with gene expression results (Fig. 5). As we wanted to compare the mean fold change of the selected genes with the expression of the IHC, we calculated the expression of the H score by multiplying the stain distribution and intensities. Though, conventionally, BRAF V600E mutation-specific stain and MMR stains are interpreted as only positive and negative, for the sake of this comparison we calculated the H scores. Correlation between these two experimental values showed similar patterns (Fig. 6).

Discussion

In this study, we planned to analyze the gene expressions commonly attributed to colonic carcinogenesis from the literature mainly in harvested ACFs compared to their expressions in CRC and normal colonic mucosa. We followed a harvesting protocol that mimics the magnified chromoendoscopic procedure to characterize them further. We found that in both ACF and CRC, multiple genes belonging to different genetic pathways were up-regulated or down-regulated, compared to the normal colonic mucosa, while some of the up-regulated and down-regulated genes in ACF and CRC were in common. Interestingly, the expression of the selected genes was not statistically different between ACF and corresponding CRC in our study. The gene expressions were correlated with tumor size, lymph node metastasis, and tumor laterality, that is, origin in the right or left colon. Protein expression analysis was performed for selected gene products due to the constrain of scant leftover tissue and showed a similar pattern of protein

expression as noted with the mRNA mean fold change. This study emphasizes the observation that even tiny, microscopic preneoplastic lesions of the colon as ACFs bear complex molecular alterations like that of a fully developed CRC, in contrast to the conventional belief of their sequential accumulation from low to higher stages.

Many researchers have attempted to study the molecular events in ACF since 1994. However, these studies fail to establish the comprehensive molecular phenotype of ACF. Our data in this study are concordant with the observation by Pretlow TP et al. that all ACF do not harbour *APC* mutation, rather *KRAS* mutation is common in them [12]. Mutations in the *KRAS* gene were the first genetic alteration detected in ACF induced in rodents [19]. According to the literature search, it appears that *CDKN2A (p16)* and *CDKN1A (p21)* cyclin-dependent kinase inhibitors are frequently inactivated in a subset of CRC, and overexpression of CDKN2A occurs in the early stage with epigenetic silencing, eventually leading to tumor progression, aberrant expression of CDKN2A and poor prognosis [20, 21]. Our findings corroborated in identifying upregulation of CDKN2A in ACF in comparison to normal colonic mucosa [22]. In previous studies, MSI-associated ACFs were identified to have histologically hyperplastic mucosa and were believed to be the precursor of hyperplastic polyp in a serrated pathway of sporadic CRC [23, 24]. We observed significant downregulation of MLH1 in ACF in comparison to normal controls, with no definite correlation of MLH1 expression between the ACF and corresponding CRC and their histologies.

A variety of inflammatory associated genes have been studied in the pathogenesis of CRC. A study by Peinado et al. suggested that these inflammatory genes are involved in the formation of a premetastatic niche required for organ-specific homing of tumor cells in CRC [25]. Wang et al. showed that the CXCR2 level is elevated in sporadic CRC and active IBD [26]. Foersch et al. stated that blocking growth factors such as VEGFR2 signalling can lead to CRC senescence and is correlated with increased patient survival [27]. Both of our inflammatory associated genes *VEGFA (p-value – 0.05) and CCL5 (p-value – 0.02)* showed statistically significant alterations in ACF. These results also corroborate the similar pathogenetic hypothesis given by Conteduca et al in 2013, stating that ACF can arise not only from major three molecular pathways but due to the amalgamation of activation of growth factors, stem cell, and chronic inflammation pathways [15].

In addition, *IGF-1*, a multifunctional peptide hormone was upregulated in ACF in this study, with its correlation with lymph node metastasis. However, the corresponding CRC included did not show *up-regulation of IGF1.* This finding contrasted with the findings of Li ZJ et al. and Shiratsuchi I et al [28, 29]. *The EGFR* gene stimulates the proliferation of neoplastic cells through the MAPK pathway and is associated with an increased pathological tumor stage [30]. Hardwick JC et al. proposed that MAPK is overexpressed and active in colorectal cells by IHC [31]. Although we identified *EGFR* upregulation in ACF, in the corresponding CRC we did not identify the same, therefore we were unable to comment on its role in colon carcinogenesis. Our study is like the previous studies which don’t show much difference in terms of molecular alteration between ACF and CRC [12, 13, 32].

No definitive correlation was found between topographic pit patterns and ACF histology and the genetic changes observed in this study. In our previous studies [9, 10], although we identified a correlation of the Zyriform pit pattern with ACF of the left colon, dysplastic histology, and TP53 expression, in the index study we did not identify any distinct correlation of topographic or histological ACF types with gene expressions. This may be either due to the low number of successful cases included in this study or it may be possible that all mucosal ACF-like lesions are genetically complex.

This study adds to the fact that ACFs can be sampled and characterized microscopically and genetically. As currently ACF-like lesions are not sampled in vivo by chromoendoscopy for screening purposes, this study was planned in fresh colectomy specimens to harvest and confirm ACF topographically and microscopically. Although FFPE tissue samples have been shown to have lower specificity and sensitivity than fresh frozen samples [17], they are an important source of material for an exploratory study such as this. Damage to nucleic acid sustained secondary to fixation, storage, and embedding processes can hamper gene expression studies, and we accept this limitation. However, the utility of automated methods adopted in this study showed good specificity (70%) and sensitivity (85%) even in FFPE samples [18]. We also did not perform laser microdissection of the ACF keeping in mind the microscopic nature of these lesions and assuming that the microdissected lesions will not produce a satisfactory amount of RNA for further analyses. We also thought this is not essential, as we assumed similar 'tumor field effects' in the ACF and its immediate adjacent mucosa. We earlier observed that the tumor field effect is observed up to a 5 cm distance of the main tumor mass; therefore, in this study, the macroscopically normal colonic mucosa was sampled from an area at least 5 cm away from the main tumor mass. However, this can be still debated. In addition, as in some of our cases, the RNA yield was low; our successful case numbers for each gene varied. Though performing western blot analysis could have given more quantifiable data, we resorted to the IHC technique keeping in mind the limited left-over tissue in the FFPE blocks already used for sectioning for RNA extraction.

To conclude, ACFs in the human colon show complex activation of pro-oncogenes, cell cycle regulator genes, apoptosis suppressor and activator genes, and inflammation regulatory genes such as the corresponding fully developed CRC. Our observation strengthens the fact that these microscopic lesions can be good candidates for screening and genetic analysis in high-risk patients by high-resolution chromoendoscopy. However, no significant correlation was observed between the topographic and histological characteristics of the ACFs & molecular changes studied; it seems that all ACF-like lesions can be sampled without worrying about their pit patterns. Further multicentre studies should strengthen our observation.

Declarations

Competing Interests:

The authors declare that they have no financial or non-financial conflict of interest.

Ethical standard: The study protocol was ethically approved by the Institute Ethics Committee.

Data availability statement: The datasets generated during and/or analysed during the current study are available from the corresponding author on reasonable request.

Acknowledgements

Funding Source: This study was supported by the Department of Biotechnology, Government of India, Grant number: 6242-P38/RGCB/PMD/DBT/PSNJ/2015.

Author contribution statement: PD & SDG conceived the study and executed the work. SM, JS, BNG, SG, RY, and LM helped to sample the shaved mucosa and to detect ACF-like lesions, histological and laboratory studies. ADU participated in the statistical analysis. VA, SP, NRD, AS & SD were involved in clinical and surgical management, supervising the work and in manuscript preparation. PD is the overall guarantor of this article.

References

1. GLOBOCAN 2020. Estimated Cancer Incidence, Mortality, and Prevalence Worldwide in 2020. http://gco.iarc.fr (December 2020).
2. NCRP. (2013) Three-year report of the population-based cancer registries- 2009–2011. National cancer registry programme, Indian council of medical research (ICMR), Bangalore, India, 2013. http://www.ncrpindia.org (November 8, 2017).
3. McVeigh TP, Lowery AJ, Waldron RM, Mahmood A, Barry K. Assessing awareness of colorectal cancer symptoms and screening in a peripheral colorectal surgical unit: a survey-based study. BMC Surg. 2013;13(1):1–7.
4. Leslie A, Carey FA, Pratt NR', Steele RJ. The colorectal adenoma-carcinoma sequence. Br J Surg. 2002;89:845–60.
5. Umar A, Srivastava S. The promise of biomarkers in colorectal cancer detection. Dis Marker. 2004;20:87–96.
6. Takayama T, Katsuki S, Takahashi Y, et al. Aberrant crypt foci of the colon as precursors of adenoma and cancer. N Engl J Med. 1998;339:1277–84.
7. Di Gregorio C, Losi L, Fante R, et al. Histology of aberrant crypt foci in the human colon. Histopathology. 1997;30:328–34.
8. Kristt D, Bryan K, Gal R. Colonic aberrant crypts may originate from impaired fissioning: Relevance to increased risk of neoplasia. Hum Pathol. 1999;30:1449–58.
9. Gupta B, Das P, Ghosh S, et al. Identification of high-risk aberrant crypt foci and mucin-depleted foci in the human colon with study of colon cancer stem cell markers. Clin Colorectal Cancer. 2017;16(3):204–13.
10. Ghosh S, Gupta B, Verma P, et al. Topographic, histological and molecular study of aberrant crypt foci identified in human colon in different clinical groups. Intestinal Res. 2018;16(1):116.

11. Hamilton SR, Vogelstein B, Kudo S, et al. Tumours of the colon and rectum. Pathology and Genetics of Tumours of the Digestive System, edited by S. R. Hamilton and L. A. Aaltonen IARC Press, Lyon, 2000, pp. 103.
12. Pretlow TP, Pretlow TG. Mutant KRAS in aberrant crypt foci (ACF): initiation of colorectal cancer? Biochim Biophys Acta. 2005;1756(2):83–96.
13. Cheng L, Lai MD. Aberrant crypt foci as microscopic precursors of colorectal cancer. World J Gastroenterol. 2003;9(12):2642–9.
14. Tariq K, Ghias K. Colorectal Cancer Carcinogenesis: A Review of Mechanisms. Cancer Biol Med. 2016;13:120–35.
15. Conteduca V, Sansonno D, Russi S, Dammacco F. Precancerous colorectal lesions. Int J Oncol. 2013;43:973–84.
16. Snover DC. Update on the serrated pathway to colorectal carcinoma. Hum Pathol. 2011;42:1–10.
17. Zhu J, Deane NG, Lewis KB. Evaluation of frozen tissue derived prognostic gene expression signatures in FFPE colorectalcancer samples. Sci Rep. 2016;6:33273.
18. Kalmar A, Wichmann B, Galamb O, et al. Gene expression analysis of normal and colorectal cancer tissue samples from frozen and matched formalin-fixed, paraffin embedded (FFPE) specimens after manual and automated RNA isolation. Methods. 2013;59:16-9.
19. Stopera SA, Murphy LC, Bird RP. Evidence for a ras gene mutation in azoxymethane-induced colonic aberrant crypts in Sprague-Dawley rats: earliest recognizable precursor lesions of experimental colon cancer. Carcinogenesis. 1992;13(11):2081-5. doi: 10.1093/carcin/13.11.2081. PMID: 1423879.
20. Herman JG, Merlo A, Mao L, et al. Inactivation of the CDKN2/p16/MTS1 gene is frequently associated with aberrant DNA methylation in all common human cancers. Cancer Res. 1995;55(20):4525–30. PMID: 7553621.
21. Cui X, Shirai Y, Wakai T, Yokoyama N, Hirano S, Hatakeyama K. Aberrant expression of pRb and p16(INK4), alone or in combination, indicates poor outcome after resection in patients with colorectal carcinoma. Hum Pathol. 2004;35(10):1189-95. doi: 10.1016/j.humpath.2004.06.010. PMID: 15492985.
22. Wang QS, Papanikolaou A, Nambiar PR, Rosenberg DW. Differential expression of p16(INK4a) in azoxymethane-induced mouse colon tumorigenesis. Mol Carcinog. 2000 Jul;28(3):139 – 47. doi: 10.1002/1098-2744(200007)28:3<139: aid-mc2 > 3.0.co;2-v. PMID: 10942530.
23. Jass JR, Whitehall VL, Young J, Leggett BA. Emerging concepts in colorectal neoplasia. Gastroenterology. 2002;123(3):862 – 76. doi: 10.1053/gast.2002.35392. PMID: 12198712.
24. Jass JR, Iino H, Ruszkiewicz A, et al. Neoplastic progression occurs through mutator pathways in hyperplastic polyposis of the colorectum. Gut. 2000;47(1):43–9. doi:10.1136/gut.47.1.43. PMID: 10861263; PMCID: PMC1727952.
25. Peinado H, Zhang H, Matei IR, et al. pre-metastatic niches: organ-specific homes for metastases. Nat Rev Cancer. 2017;17(5):302–17. doi:10.1038/nrc.2017.6. Epub 2017 Mar 17. PMID: 28303905.

26. Wang D, Dubois RN, Richmond A. The role of chemokines in intestinal inflammation and cancer. Curr Opin Pharmacol. 2009;9(6):688–96. doi:10.1016/j.coph.2009.08.003. Epub 2009 Sep 4. PMID: 19734090; PMCID: PMC2787713.
27. Foersch S, Sperka T, Lindner C, et al. VEGFR2 Signaling Prevents Colorectal Cancer Cell Senescence to Promote Tumorigenesis in Mice with Colitis. Gastroenterology. 2015;149(1):177–89. .e10 . doi: 10.1053/j.gastro.2015.03.016. Epub 2015 Mar 19. PMID: 25797700.
28. Li ZJ, Ying XJ, Chen HL, et al. Insulin-like growth factor-1 induces lymphangiogenesis and facilitates lymphatic metastasis in colorectal cancer. World J Gastroenterol. 2013;19(43):7788–94. doi:10.3748/wjg.v19.i43.7788. PMID: 24282367; PMCID: PMC3837280.
29. Shiratsuchi I, Akagi Y, Kawahara A, et al. Expression of IGF-1 and IGF-1R and their relation to clinicopathological factors in colorectal cancer. Anticancer Res. 2011;31(7):2541-5. PMID: 21873172.
30. Huang CW, Tsai HL, Chen YT, et al. The prognostic values of EGFR expression and KRAS mutation in patients with synchronous or metachronous metastatic colorectal cancer. BMC Cancer. 2013;13:599. https://doi.org/10.1186/1471-2407-13-599.
31. Hardwick JC, van den Brink GR, Offerhaus GJ, van Deventer SJ, Peppelenbosch MP. NF-kappaB, p38 MAPK, and JNK are highly expressed and active in the stroma of human colonic adenomatous polyps. Oncogene. 2001;20(7):819 – 27. doi: 10.1038/sj.onc.1204162. PMID: 11314016.
32. Perse M, Cerar A, "Morphological and molecular alterations in 1,2 dimethylhy drazine and azoxymethane induced colon carcinogenesis in rats," J. Biomed. Biotechnol., Vol. 2011, 2011, pp. 473964.

Figures

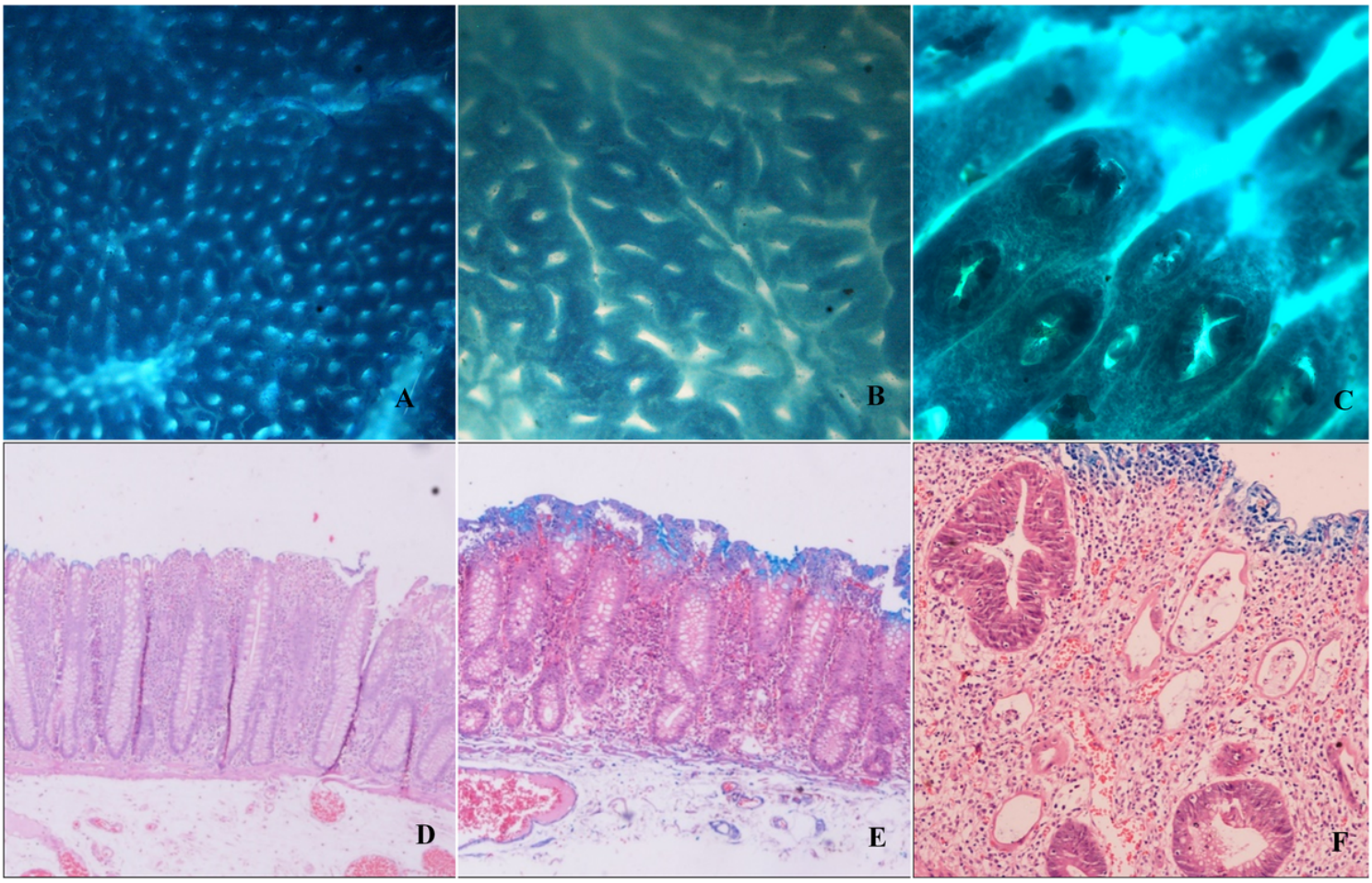

Figure 1

Topographic images of ACF. A shows ACF with round pits, B shows ACF with slit-shaped pits, and C shows ACF with gyriform pits. D shows ACF with normal epithelial lining (x 40), E shows ACF with hyperplastic epithelial lining (x 40) and F shows ACF with dysplastic epithelial lining (X 100).

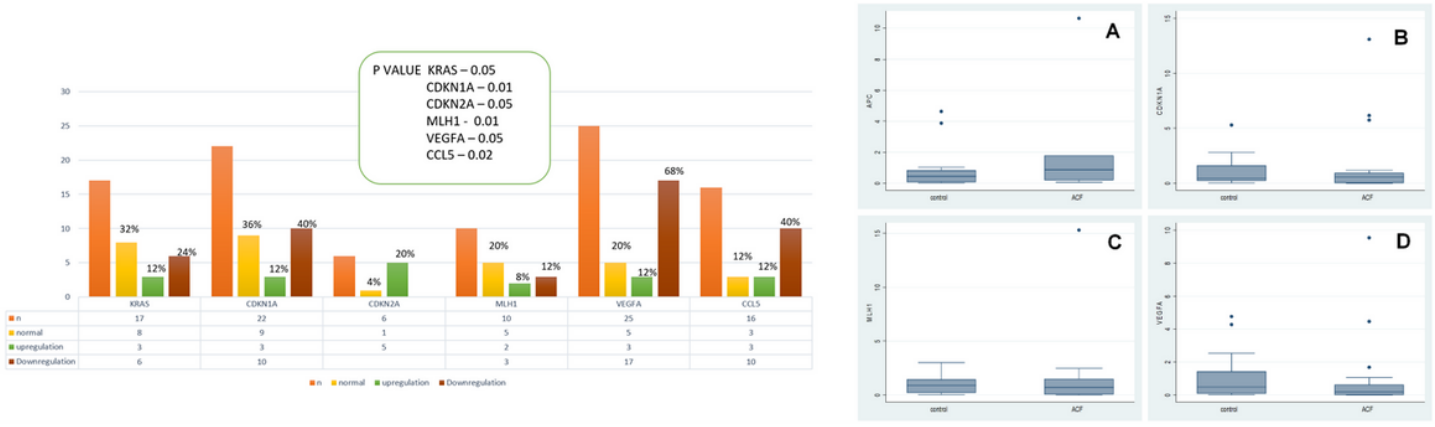

Figure 2

The bar diagram shows a summary of the fold change of genes studied in control versus ACFs. Box and whisker graphs showing the comparison of *APC* (A, MFC 2.22, p-value 0.396), *CDKN1A* (B, MFC 1.51, p-value 0.01), *MLH1* (C, MFC 2.24, p-value 0.01) and *VEGFA* (D, MFC 0.87, p-value 0.05) between control and ACF. *(MFC- mean fold change)*

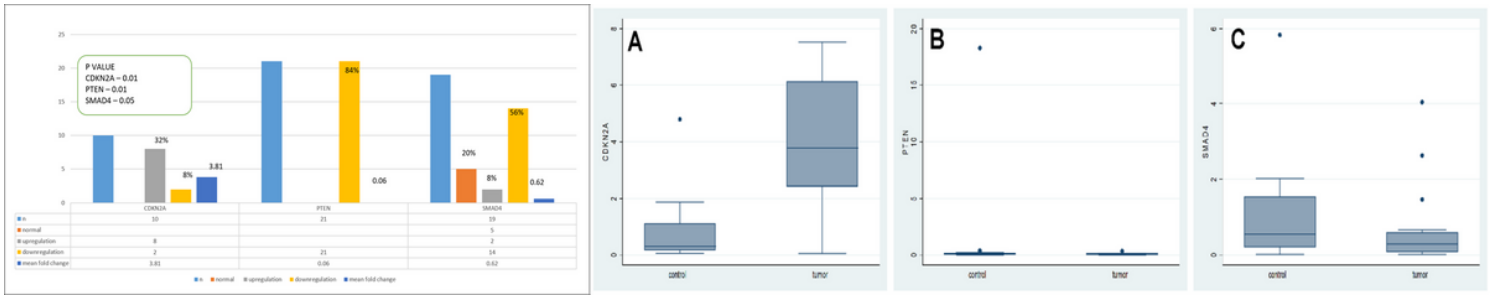

Figure 3

The bar diagram shows a summary of the fold change of genes studied in control versus CRC. Box and whisker graphs showing the comparison of *CDKN2A* (A, MFC 3.81, p-value 0.01), *PTEN* (B, MFC 0.06, p-value 0.01), and the *SMAD4 gene* (C, MFC 0.62, p-value 0.05) between control and CRC. *(MFC- mean fold change)*

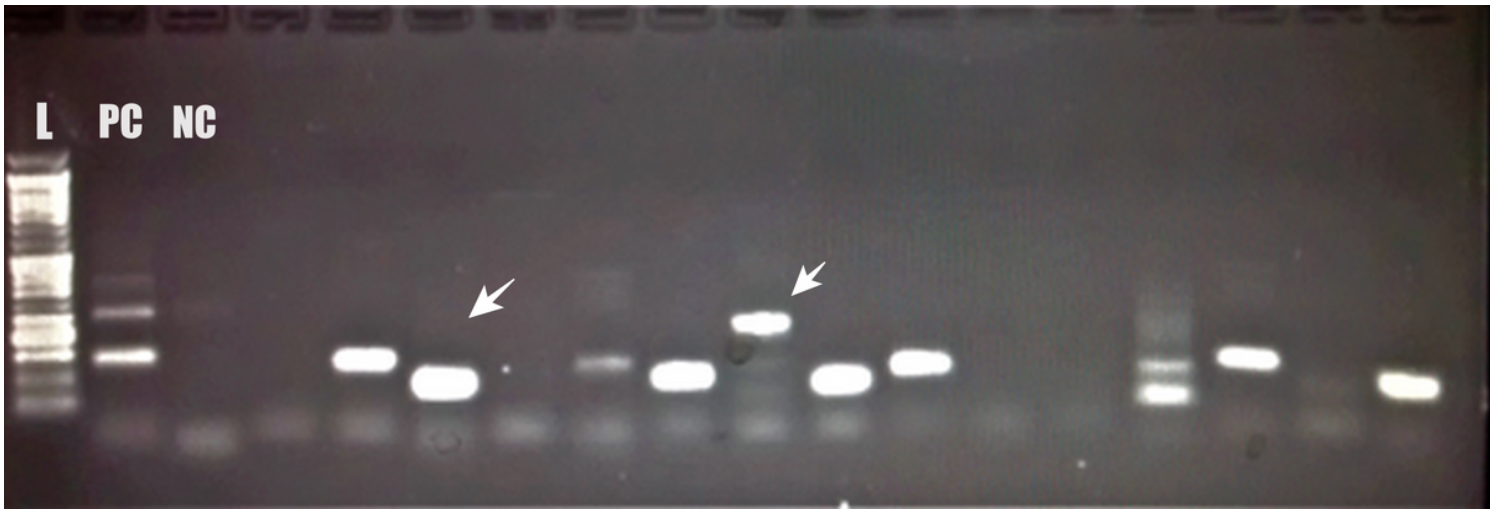

Figure 4

Agarose gel electrophoresis [2% agarose gel run in 0.5 x TBE and stained with ethidium bromide (EtBr)] shows different specific post-PCR amplicons in different columns (arrows), positive control (PC), and negative controls (NC) compared to the reference ladder (L, 120-130bp).

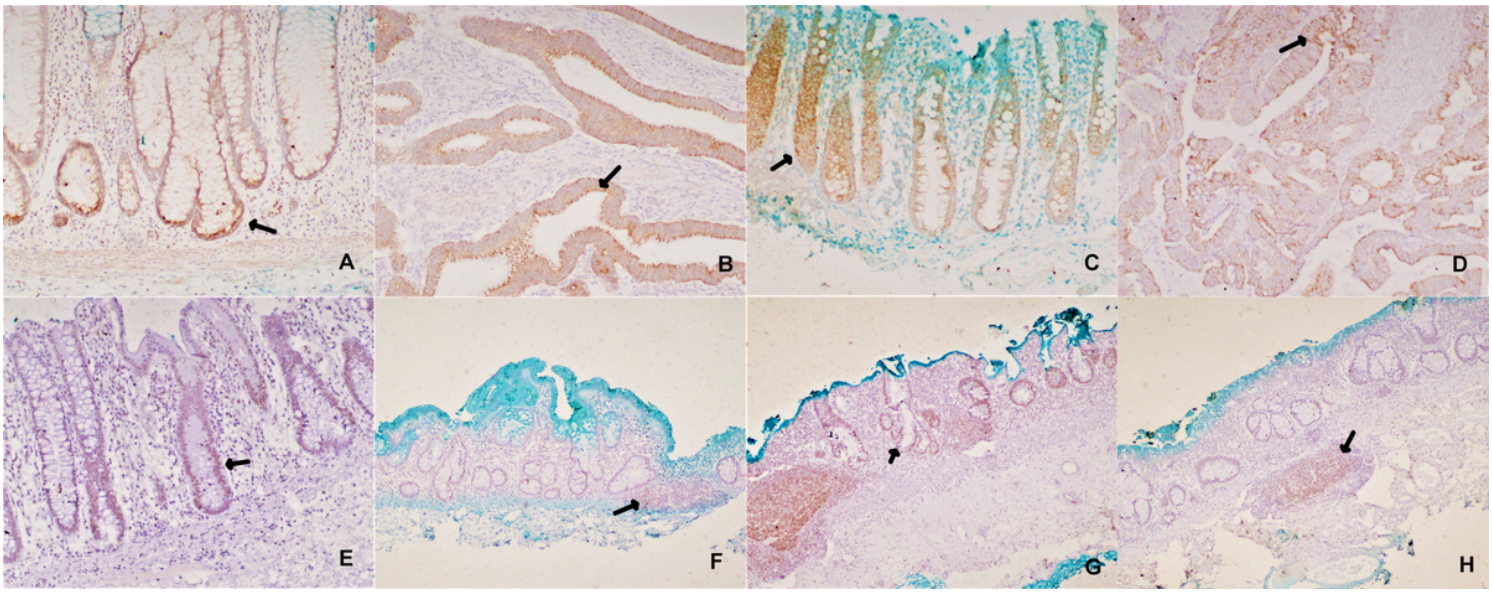

Figure 5

Immunohistochemical staining for APC is seen in ACF (A, arrow x 200) and the corresponding CRC (arrow, b x 100). BRAFV600E mutation-specific stain shows positivity in the ACF (C, arrow x 100) and corresponding CRC (D, arrow x 200). MLH1 stain shows retained nuclear positivity in one ACF (arrow, E x 100), while another ACF shows loss of MLH1. The positivity in lymphocytes can be identified (F, arrow x 40). The PMS2 stain shows retained nuclear positivity in one ACF (arrow, G x100), while another ACF shows nuclear loss. The positivity in lymphocytes can be identified (arrow, H x100).

Figure 6

The bar diagrams represent H scores calculated on a few immunohistochemical stains performed, and the mean fold change values of the corresponding genes performed in this study.